Amphisome plays a role in HBV production and release through the endosomal and autophagic pathways

VISUAL ABSTRACT

Amphisome plays a role in HBV production and release through the endosomal and autophagic pathways

Background

- Autophagic and endosomal pathways coordinately contribute to hepatitis B virus (HBV) virion and subviral particle (SVP) production.
- GW4869 inhibits MVB function and exosome secretion by inhibiting ceramide-mediated inward membrane budding.
- RAB27 is a small GTPase involved in the regulation of exosome release.

Findings

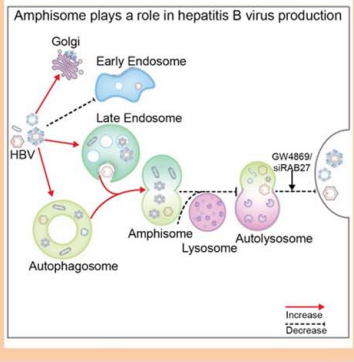

Conclusion

GW4869 treatment and RAB27 silencing increase the fusion of autophagosomes with MVBs to form amphisomes and retain HBV in amphisomes, resulting in decreased HBV particle secretion. This process demonstrates the amphisomes' potential role as a platform for HBV release.

Received: 1 August 2024 | Accepted: 8 January 2025

DOI: 10.1097/HC9.0000000000000654

ORIGINAL ARTICLE

OPEN

Amphisome plays a role in HBV production and release through the endosomal and autophagic pathways

Jia Li[1] | **Thekla Kemper**[1] | **Ruth Broering**[2] | **Yong Lin**[3] | **Xueyu Wang**[1] | **Mengji Lu**[1]

[1]Institute for Virology, University Hospital Essen, University of Duisburg-Essen, Essen, Germany

[2]Department of Gastroenterology, Hepatology and Transplant Medicine, University Hospital Essen, University of Duisburg-Essen, Essen, Germany

[3]The Key Laboratory of Molecular Biology of Infectious Diseases Designated by the Chinese Ministry of Education, Chongqing Medical University, Chongqing, China

Correspondence
Mengji Lu, Institute for Virology, University Hospital Essen, Hufelandstrasse 55, Essen 45122, Germany.
Email: mengji.lu@uni-due.de

Abstract

Background: Autophagic and endosomal pathways coordinately contribute to HBV virions and subviral particles (SVPs) production. To date, limited evidence supports that HBV and exosomes have a common pathway for their biogenesis and secretion. The final steps of HBV production and release have not yet been well studied.

Methods: We examined the production and release of HBV virions and SVPs by using GW4869 (N,N'-Bis[4-(4,5-dihydro-1H-imidazol-2-yl)phenyl]-3,3'-pht hal amide dihydrochloride), a small molecule inhibiting ceramide-mediated inward membrane budding. Neutral sphingomyelinase, the target of GW4869, and RAB27A and –B, 2 small GTPases involved in exosome release control, were silenced using gene silencing to confirm the results obtained. Western blot, immunofluorescence staining, and confocal microscopy were applied.

Results: GW4869 inhibited HBV virion release, causing their accumulation along with SVPs in hepatocytes. This triggered cellular endoplasmic reticulum stress, leading to protein kinase B-mechanistic target of rapamycin kinase signaling pathway inactivation. GW4869 treatment increased autophagosome formation and impaired autophagic degradation by blocking autophagosome-lysosome fusion. Consequently, HBsAg is increasingly localized to autophagosomes and late endosomes/multivesicular bodies. Silencing neutral sphingomyelinase yielded consistent results. Similarly, RAB27A silencing inhibited HBV virion and SVP secretion, causing their accumulation within hepatoma cells. Notably, GW4869 treatment, as well as RAB27A and -B silencing, increased the presence of $LC3^{+}CD63^{+}HBsAg^{+}$ complexes.

Abbreviations: AKT-MTOR, protein kinase B- mechanistic target of rapamycin kinase; ER, endoplasmic reticulum; EVs, extracellular vesicles; GW4869, N,N'-Bis[4-(4,5-dihydro-1H-imidazol-2-yl)phenyl]-3,3'-pht hal amide dihydrochloride; IF, immunofluorescence; LAMP1, lysosomal-associated membrane protein 1; MVBs, multivesicular bodies; nSMase, neutral sphingomyelinase; PHH, primary human hepatocyte; pSM2, an HBV replication-competent plasmid; siRNA, small interfering RNA; SMPD2, sphingomyelin phosphodiesterase 2; SVP, subviral particle; ULK1, UNC-51-like kinase 1.

Supplemental Digital Content is available for this article. Direct URL citations are provided in the HTML and PDF versions of this article on the journal's website, www.hepcommjournal.com.

Conclusions: Our results demonstrate the involvement of the autophagosome-late endosome/multivesicular bodies-exosome axis in regulating HBV production and release, highlighting amphisomes as a potential platform for HBV release.

Keywords: autophagic process, endosomal trafficking, GW4869, HBV, RAB27A/B

INTRODUCTION

HBV causes acute and chronic hepatitis B, which may result in severe liver diseases. Chronic HBV infection increases the risk of liver cirrhosis and HCC.[1] The complete HBV virion consists of a nucleocapsid and an envelope with 3 HBsAgs: small (S), middle (M), and large (L). The HBV capsids consist of a core protein (HBcAg), and a relaxed circular, partially dsDNA genome is packaged in the icosahedral symmetry structure. In addition, noninfectious subviral particles (SVPs) are only produced and secreted in spherical and filamentous forms.[2] Yet, the mechanisms governing the envelopment and release of HBV virions and SVPs within cellular compartments remain incompletely elucidated.

Infectious HBV virions and various incomplete viral particles, including SVPs, naked nucleocapsids, and empty virions, can be released from hepatocytes. These distinct HBV components utilize diverse pathways for their secretion.[3] Spheres are released through the constitutive secretory pathway, while HBV virions and filamentous SVPs are secreted through the endosomal pathway.[4,5] Autophagy also represents a pathway for HBV assembly and can be induced to substantially enhance HBV production, for example, by the mechanistic target of rapamycin kinase (MTOR) inhibitor rapamycin.[6] Autophagosomes might fuse with lysosomes, clearing cellular components through lysosomal degradation. However, a part of them may escape lysosomal degradation and release their cargo into the extracellular environment in a yet undefined mechanism. Our latest study demonstrated that autophagy could promote HBV replication and production only when endosomal trafficking is partially functional,[7] hinting that the interconnection of late endosomes/multivesicular bodies (MVBs) and autophagosomes to form amphisomes facilitates HBV production.

Exosomes are extracellular vesicles (EVs) released by late endosomes/MVBs of 40–160 nm in size. Prior investigations have detected HBV DNA, RNA, and HBV proteins associated with exosomes derived from HBV-infected hepatocytes.[8,9] Hence, the inhibition of EV formation and secretion may impede HBV release. Several pharmacological inhibitors targeting lipid metabolism and EV trafficking also block MVB function and EV secretion.[10] Notably, GW4869 (N,N'-Bis[4-(4,5-dihydro-1H-imidazol-2-yl)phenyl]-3,3'-pht hal amide dihydrochloride) is a widely used MVB inhibitor that inhibits neutral sphingomyelinases (nSMases), leading to a reduction of exosome secretion. GW4869 inhibits HBV virion secretion by disturbing MVB or exosome formation.[8] GW4869 could reduce HBV transmission and liver fibrosis by suppressing the production of HBV-DNA–containing or miR-222–containing exosomes.[9,11] Nonetheless, the precise mechanisms underlying GW4869's interference with late endosome/MVB function and its effects on HBV trafficking within cells remain elusive. RAB27 also regulates exosome secretion.[12] It has been observed that the cellular escape of HCV[13] and HEV[14] depends on Rab27A. Whether HBV utilizes this Rab protein for cellular escape remains to be determined.

This study investigated the mechanisms of GW4869, RAB27A, and -B in HBV trafficking, providing insights into the roles of autophagosome-late endosome/MVB-exosome axis and amphisome in HBV replication and release.

METHODS

Cell culture and transfection

In this study, we used 3 standard HBV replication cell models: HepG2.2.15 cells, a cell line with stable and constant HBV replication; Huh7 cells transfected with HBV plasmid, a transient HBV replication cell model; and HBV-infected primary human hepatocytes (PHHs). All used cell lines were cultured at 37°C in a humidified environment containing 5% CO_2. HepG2.2.15 human hepatoma cells, harboring integrated dimers of the HBV genome (GenBank accession number, U95551), were cultured in RPMI 1640 medium (Gibco, 11875093), supplemented with 10% inactivated fetal bovine serum (Gibco, 10270106), 100 U/mL of penicillin (Gibco, 15140122), 100 μg/mL of streptomycin (Gibco, 15140122), 1% nonessential amino acids (Gibco, 111500500), 1% HEPES (Gibco, 15630080), and 500 μg/mL of G418 (ITW Reagents, A6798). Another hepatoma cell line Huh7 was grown in DMEM medium (Gibco, 41966029), supplemented with 10% inactivated

fetal bovine serum, 100 U/mL of penicillin, 100 μg/mL of streptomycin, 1% nonessential amino acids, and 1% HEPES. PHHs were grown in William's E Medium (PAN-biotech, P0429050), supplemented with 250 μL of insulin (Sigma-Aldrich, I–034), 2% DMSO (Sigma-Aldrich, D5879), 125 μL of hydrocortisone hemisuccinate (Sigma-Aldrich, 1319002), and 100 U/mL of penicillin, 100 μg/mL of streptomycin. Transfection of plasmid or small interfering RNAs (siRNAs) was performed by using Lipofectamine 2000 transfection reagent (Invitrogen, 11668019) according to the manufacturer's instructions.

Statistical analysis

Results are shown as the means ± SEM. Statistical analyses were performed using GraphPad Prism software (version 8; GraphPad Software Inc). The difference of means between the 2 groups was determined by the Student paired *t* test. Data for single-factor experiments were performed using the 1-way ANOVA procedure. $p < 0.05$ was considered statistically significant and indicated by asterisks or pounds. All experiments were repeated independently at least 3 times.

See Supplemental Materials, http://links.lww.com/HC9/B910 (Table 1), for details regarding western blot, HBV gene expression and replication, immunofluorescence staining, colocalization calculation, lysosomal activity detection, exosome isolation, and cell proliferation assay.

RESULTS

GW4869 treatment blocks HBV virion secretion and sequesters SVPs and virions within cells

To investigate the impact of exosome biogenesis inhibition on HBV release, we individually tested 5 different small molecules—calpeptin, Y27632, GW4869, imipramine, and endosidin2—targeting endosomal membrane trafficking or lipid metabolism.[15] These compounds showed diverse effects on endosome and autophagic functions and HBV replication (Supplemental Figure S1, http://links.lww.com/HC9/B910). The significantly altered ratio between the intracellular and extracellular HBV DNA levels after GW4869 treatment was particularly interesting. Consequently, we conducted detailed examinations of GW4869's effects on HBV production and release.

HepG2.2.15 cells, Huh7 cells, and PHHs were cultured with varying concentrations of GW4869, ranging from 1 to 10 μM. Cell viability was monitored by the cell counting kit-8 assay and beta-actin detection by western blot (Supplemental Figure S2, http://links.lww.com/HC9/B910). Subsequently, GW4869 concentrations below 5 μM for HepG2.2.15 cells and 2 μM for Huh7 cells were selected. All experiments involving Huh7 cells were analyzed at 48 hours to minimize undesired effects on cell growth.

We examined the effects of GW4869 on HBV gene expression and replication. 5 μM GW4869 treatment effectively decreased HBV DNA levels in the culture supernatants at the early time point (Supplemental Figure S3, http://links.lww.com/HC9/B910). Prolonged treatment with GW4869 for 72 hours led to a strong dose-dependent increase in intracellular HBV DNA levels in HepG2.2.15 cells. The total secreted HBV DNA and HBV virion-associated DNA levels were significantly decreased. Both intracellular and extracellular HBsAg levels were increased. The total HBV RNA levels remained unchanged (Figure 1A).

In addition to the stable HBV replication cell model, we utilized other de novo HBV replication cell models. Huh7 cells were transiently transfected with an HBV replication-competent plasmid (pSM2) and then treated with GW4869 at a concentration of 1 μM for 48 hours (Figure 1B). Consistently, intracellular HBV DNA levels markedly increased and decreased secreted HBV virion-associated DNA levels after GW4869 treatment. GW4869 had little to no effects on intracellular and extracellular HBsAg and total HBV RNA levels at the given concentration. We also treated HepG2.2.15 and Huh7 cells with medium replenished every 24 hours with GW4869. Under this condition, GW4869 treatment consistently increased the levels of secreted HBsAg, similar to the incubation over 72 hours without medium changes (Supplemental Figure S4, http://links.lww.com/HC9/B910).

Finally, PHHs were infected with HBV and treated with 5 μM of GW4869 for 48 hours. Secreted HBV DNA, HBsAg, and HBeAg levels decreased, while total intracellular HBV RNA levels tended to be slightly higher but without statistical significance after GW4869 treatment (Figure 1C). Consistently, confocal microscopy and western blot analysis demonstrated a significant increase in HBV protein expression levels in HepG2.2.15 and pSM2-transfected Huh7 cells (Figure 1D). Although HBsAg expression was significantly increased in single cells in the Huh7 cell culture, the total intracellular HBsAg amount increased only slightly due to slightly reduced cell growth after GW4869 treatment. Altogether, GW4869 treatment led to the intracellular accumulation of encapsidated HBV DNA and a reduction in HBV virion release.

GW4869 induces endoplasmic reticulum stress and inactivation of the AKT-MTOR signaling pathway

HBV infection induces endoplasmic reticulum (ER) stress, which in turn triggers cellular autophagy to facilitate HBV replication and production.[15,16] To

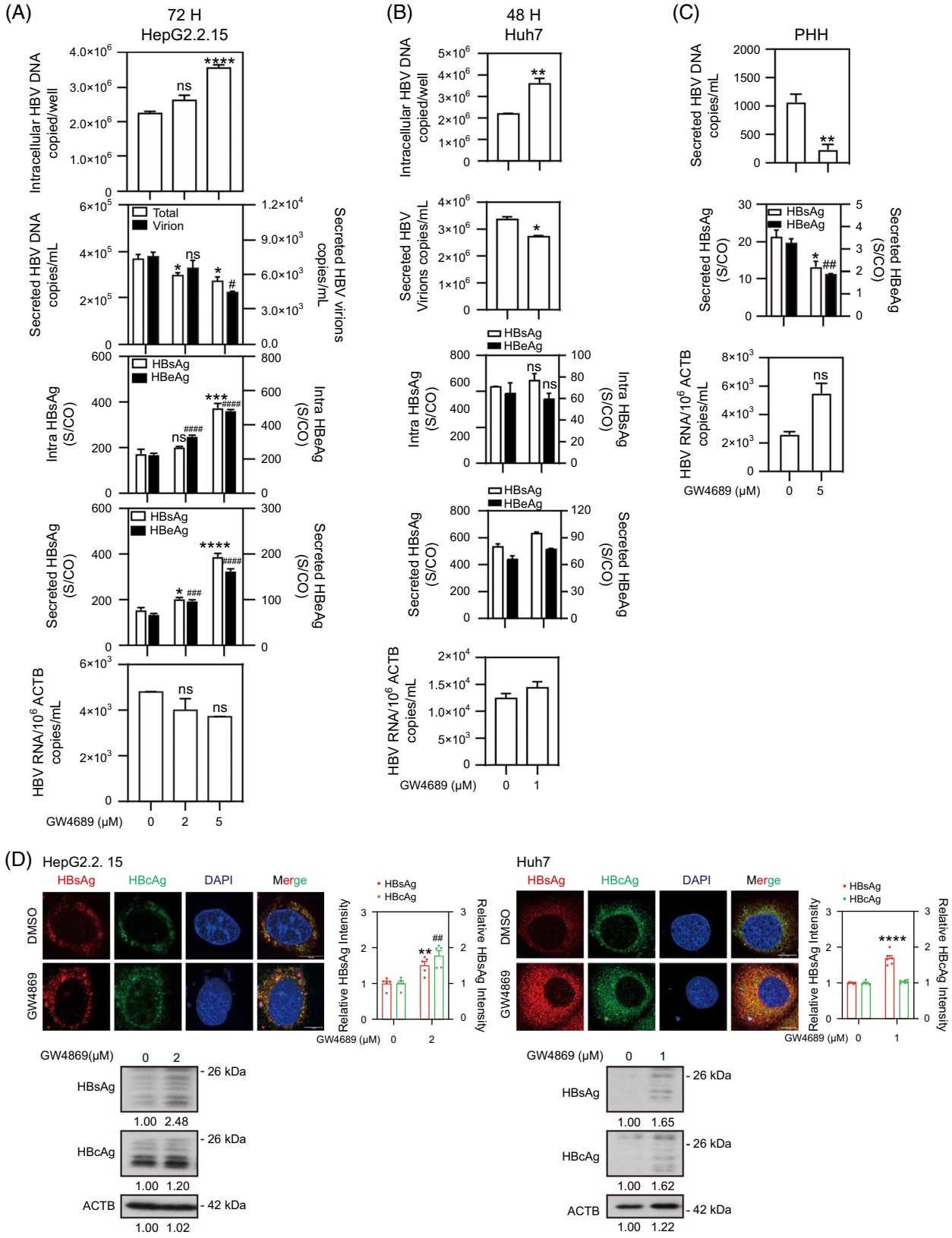

FIGURE 1 GW4869 treatment blocks HBV virion secretion and sequesters SVPs and virions within cells. (A) HepG2.2.15 cells were treated with 2 and 5 μM GW4869 for 72 hours. (B) Huh7 cells were transfected with pSM2. Six hours posttransfection, the cells were treated with 1 μM GW4869 for 48 hours. (C) PHHs were infected with purified HBV particles (MOI = 30). Eight days after infection, PHHs were treated with 5 μM GW4869 for 48 hours. The levels of intracellular HBV DNA, secreted total HBV DNA and secreted virions, the levels of intracellular and secreted HBsAg and HBeAg, and total HBV RNAs were measured. (D) HepG2.2.15 cells were treated with 2 μM GW4869 for 48 hours. pSM2-transfected

Huh7 cells were treated with 1 μM GW4869 for 48 hours. The expression levels of HBsAg and HBcAg were assessed by IF staining and western blot. The fluorescence intensity was analyzed using ImageJ software. The relative levels of indicated proteins were determined by quantifying the gray scales of bands using ImageJ software and ACTB as a loading control. Scale bar: 10 μm. $^{*,\ \#}p < 0.05$; $^{**,\ \#\#}p < 0.01$; $^{***,\ \#\#\#}p < 0.001$; $^{****,\ \#\#\#\#}p < 0.0001$; and ns, not significant. Abbreviations: ACTB, beta-actin; IF, immunofluorescence; GW4869, N,N'-Bis[4-(4,5-dihydro-1H-imidazol-2-yl)phenyl]-3,3'-pht hal amide dihydrochloride; MOI, multiplicity of infection; PHH, primary human hepatocytes; pSM2, HBV replication-competent plasmid; SVP, subviral particle.

explore whether GW4869-induced HBsAg accumulation was localized in the ER compartment, we used immunofluorescence (IF) staining and confocal microscopy. The fluorescence intensity of protein disulfide isomerase, an identified marker of ER, was increased. PDI^+HBsAg complex increased from 5.3% to 12.1% after GW4869 treatment (Figure 2A). These results indicate that GW4869 treatment results in ER expansion and the accumulation of HBsAg within ER.

We then asked whether ER stress was triggered by the HBV protein accumulation. The ER stress-related markers, including immunoglobulin binding protein /78-kDa glucose-regulated protein, total and phosphorylated eukaryotic initiation factor 2A, and activating transcription factor 6, were detected by western blot. GW4869 alone could not induce ER stress in the absence of HBV infection (Figure 2B). However, GW4869 significantly increased ER stress (Figure 2C) in HepG2.2.15 cells, HBV-transfected huh7 cells, and HBV-infected PHHs. Thus, GW4869 triggers ER stress in a feedback loop through the accumulation of HBsAg.

HBV infection and increased ER stress can disrupt the activation of the protein kinase B- mechanistic target of rapamycin kinase (AKT-MTOR) signaling pathway.[15] Thus, we assessed the levels of total and phosphorylated AKT and MTOR, as well as their downstream molecules ribosomal protein S6 Kinase B1 and UNC-51-like kinase 1 (ULK1), by western blot (Figure 2D). GW4869 decreased the levels of total and phosphorylated AKT, MTOR, and ribosomal protein S6 Kinase B1 in HepG2.2.15 cells, especially at a GW4869 concentration of 5 μM. It decreased total ULK1 levels but upregulated the p-ULK1 levels. These results demonstrated the inhibition of the AKT-MTOR signaling pathway by GW4869 treatment. Consistently, decreased levels of phosphorylated AKT and MTOR, along with increased phosphorylated ULK1 levels, were also observed in Huh7 cells and PHHs. Thus, GW4869 inhibits the AKT-MTOR signaling pathway.

GW4869 increases the formation of autophagosomes but prevents autophagic degradation by inhibiting autophagosome-lysosome fusion

Increased ER stress and the inhibition of the AKT-MTOR signaling pathway have been associated with the induction of cellular autophagy.[15,17] In light of this, we hypothesized that GW4869 treatment might augment cellular autophagy. Western blot analysis revealed an accumulation of sequestosome 1 and LC3-II proteins in GW4869-treated HepG2.2.15 cells in a dose-dependent manner (Figure 3A). Correspondingly, IF staining indicated increased sequestosome 1 levels, an elevated number of LC3-positive puncta, and heightened LC3 fluorescence intensity, suggesting decreased cargo degradation and increased autophagy levels (Figure 3B). To directly verify the reduced autophagic degradation, we conducted a Dye Quenched-Red Bovine Serum Albumin trafficking assay. Typically, Dye Quenched-Red Bovine Serum Albumin undergoes uptake, transportation to lysosomes, and subsequent cleavage by lysosomal hydrolases, resulting in robust red fluorescence. However, GW4869 remarkably reduced Dye Quenched-Red Bovine Serum Albumin-derived fluorescence, suggesting decreased cargo degradation by lysosomes (Figure 3C).

This observation prompted an investigation into the underlying cause of reduced lysosomal degradation. Drawing on prior studies, we considered 2 plausible explanations. To assess lysosomal enzymatic activity, we used the fluorescence dyes LysoTracker Red and acridine orange. The fluorescence intensities of LysoTracker Red (Figure 3D) or acridine orange (Figure 3E) in cells showed no significant changes with the GW4869 treatment, indicating preserved lysosomal enzymatic activity. Consequently, we hypothesized that GW4869 might impede lysosomal degradation by preventing autophagosome-lysosome fusion. To evaluate this hypothesis, we analyzed the colocalization of autophagosome and lysosome markers, LC3 and lysosomal-associated membrane protein 1 (LAMP1). GW4869 decreased the $LAMP1^+\ LC3^+$ complexes from 24% to 18% (Figure 3F), proving that GW4869 treatment impaired autophagosome-lysosome fusion and increased autophagosome accumulation. These findings collectively demonstrate that GW4869 prevents autophagic degradation by reducing the fusion of autophagosomes with lysosomes without alteration in lysosome enzymatic activity.

GW4869 treatment promotes the association of HBV virions and SVPs with late endosomes/MVBs and autophagosomes

Mechanistically, GW4869 inhibits ceramide-mediated inward budding of membranes, thereby impairing the

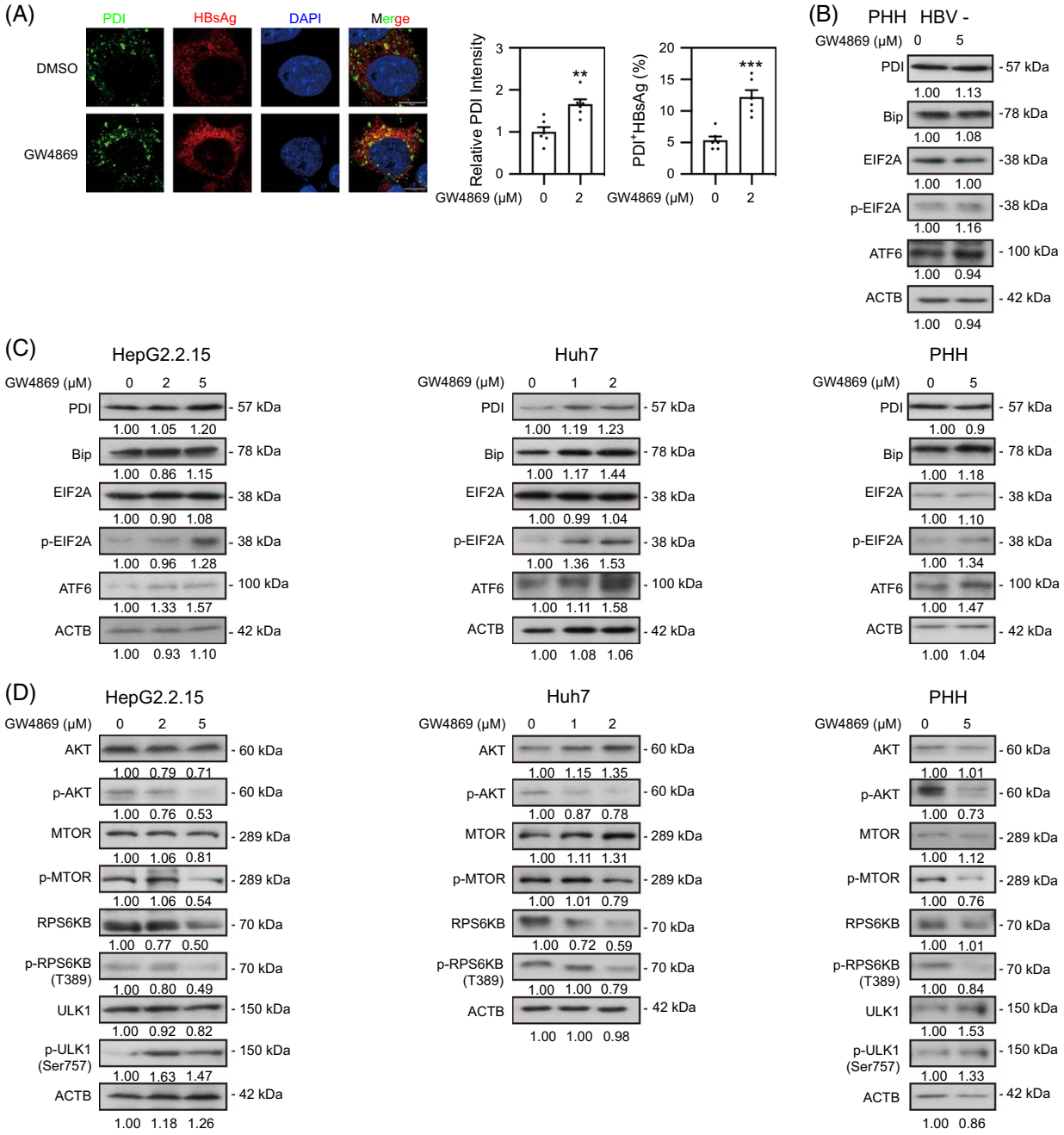

FIGURE 2 GW4869 treatment induces ER stress and the inactivation of AKT/MTOR in hepatic cells. (A) HepG2.2.15 cells were treated with 2 μM GW4869 for 48 hours. The expression levels of PDI and its colocalization with HBsAg were detected by IF staining and confocal microscopy. Scale bar: 10 μm. (B) PHHs were treated with 5 μM GW4869 and harvested after 48 hours. (C) HepG2.2.15 cells, pSM2-transfected Huh7 cells, and HBV-infected PHHs were treated with GW4869 for 48 hours. The levels of PDI, Bip, EIF2A, p-EIF2A, ATF6, (D) and AKT, MTOR, RPS6KB, ULK1, and their corresponding phosphorylated forms were detected by western blot. The relative levels of indicated proteins were determined by quantifying the gray scales of bands using ImageJ software and ACTB as a loading control. $^{**}p < 0.01$; $^{***}p < 0.001$. Abbreviations: ACTB, beta-actin; ATF6, activating transcription factor 6; Bip, immunoglobulin binding protein; EIF2A, eukaryotic translation initiation factor 2A; ER, endoplasmic reticulum; IF, immunofluorescence; GW4869, N,N'-Bis[4-(4,5-dihydro-1H-imidazol-2-yl)phenyl]-3,3'-pht hal amide dihydrochloride; MTOR, mechanistic target of rapamycin kinase; PDI, protein disulfide isomerase; PHH, primary human hepatocytes; pSM2, HBV replication-competent plasmid; RPS6KB, ribosomal protein S6 Kinase B1; ULK1, UNC-51-like kinase 1.

formation of late endosomes/MVBs and the release of mature exosomes from MVBs.[10] We explored the effects of GW4869 treatment on endosome formation within HepG2.2.15 cells. GW4869 decreased the expression levels of RAB5A and its effector, early endosome Ag 1. While the expression levels of late endosome/MVB markers CD63 and CD81 remained largely unaffected, lysosome levels significantly increased (Figure 4A). IF staining consistently showed lower fluorescence intensity of RAB5A and fewer RAB5A$^+$HBsAg$^+$ complexes

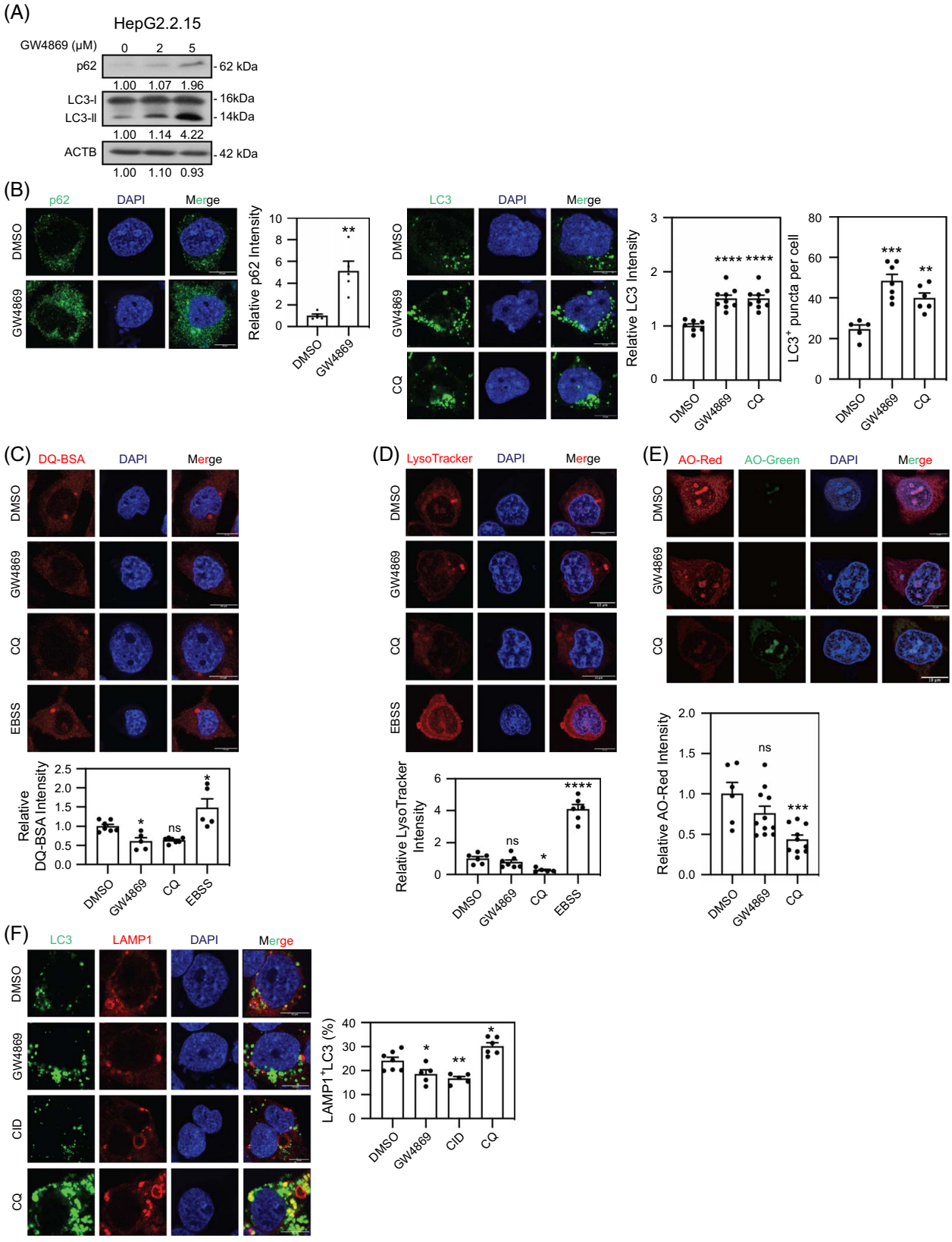

FIGURE 3 GW4869 increases the formation of autophagosomes and prevents autophagic degradation from autophagosome-lysosome fusion. (A) HepG2.2.15 cells were treated with 2 and 5 μM GW4869. The levels of p62 and LC3 were detected by western blot. The relative levels of indicated proteins were determined by quantifying the gray scales of bands using ImageJ software and ACTB as a loading control. (B) HepG2.2.15 cells were treated with 2 μM GW4869 for 48 hours, and the expression levels of p62 and LC3 were assessed by IF staining. Cells

were treated with 10 μM CQ for 24 hours as a positive control. (C) HepG2.2.15 cells were treated with 2 μM of GW4869 for 48 hours, followed by incubation with 10 mg/mL of DQ-BSA for 30 minutes, (D) 100 nM of LysoTracker Red for 1 hour, (E) and 5 μM of AO for 15 minutes. Cells treated with 10 μM of CQ for 24 hours or incubated with EBSS for 2 hours were used as controls. The fluorescence signals were analyzed. (F) HepG2.2.15 cells were treated with 2 μM of GW4869 for 48 hours. Cells cultured with 5 μM of CID or 10 μM of CQ for 24 hours were used as controls. The colocalization of LC3 and LAMP1 was analyzed using ImageJ software. Scale bar: 10 μm. $^{*}p < 0.05$; $^{**}p < 0.01$; $^{***}p < 0.001$; $^{****}p < 0.0001$; and ns, not significant. Abbreviations: ACTB, beta-actin; AO, acridine orange; CID, CID-2011756; CQ, chloroquine; DQ-BSA, Dye Quenched-Bovine Serum Albumin; EBSS, Earle's balanced salt solution; IF, immunofluorescence; GW4869, N,N'-Bis[4-(4,5-dihydro-1H-imidazol-2-yl)phenyl]-3,3'-pht hal amide dihydrochloride); LAMP1, lysosomal-associated membrane protein 1; p62, sequestosome 1.

following GW4869 treatment (Figure 4B), suggesting impaired early endosome formation and the prevention of HBsAg entry. GW4869 treatment prominently enhanced $CD63^{+}HBcAg^{+}$ complexes (from 8.6% to 15.6%) but did not affect $CD63^{+}HBsAg^{+}$ structure, indicating the prevention of HBcAg release from late endosomes/MVBs (Figure 4C). The decreased early endosomes did not logically inhibit late endosome formation. Morphologically, late endosomes/MVBs exhibited a dotted band under standard culture conditions but appeared more unstructured after GW4869 treatment (Supplemental Figure S5, http://links.lww.com/HC9/B910). GW4869 treatment also significantly increased the number of $LC3^{+}HBsAg$ and $LC3^{+}HBcAg$ complexes (Figure 4D), implying redirection of HBV proteins toward autophagosomes. GW4869 treatment decreased the colocalization of HBsAg and LAMP1 (from 16% to 10%) (Figure 4E), suggesting hindered degradation of HBsAg likely accountable for its intracellular accumulation.

In a parallel approach, Huh7 cells were transfected with pSM2 and then treated with 1 μM GW4869 for 48 hours. Consistent with the results obtained in HepG2.2.15 cells, the GW4869 treatment led to a decrease in the RAB5A expression level but an increase in the LC3 expression level. The colocalization ratio of HBsAg with RAB5A was reduced, while that of HBsAg with LC3 increased (Supplemental Figure S6, http://links.lww.com/HC9/B910).

Overall, GW4869 impaired late endosome functionality, engendering negative feedback on endosomal trafficking but concurrently stimulating autophagy. It disturbed the trafficking of HBsAg to early endosomes but reserved the HBV proteins within the late endosomes/MVBs and autophagosomes.

$LC3^{+}CD63^{+}$ amphisome-like structure acts as a platform for HBV secretion

Amphisomes, intermediate organelles resulting from the fusion of autophagosomes with late endosomes/MVBs, function in cargo degradation and secretion.[18–20] Thus, we used $LC3^{+}CD63^{+}$ as the autophagosome marker and analyzed their possible association with HBsAg. As shown in Figures 5A and B, GW4869 increased the intensity of $CD63^{+}$ LC3, indicating the promotion of late endosomes/MVBs fusion with autophagosomes, thereby leading to amphisome formation. GW4869 also increased the number of $HBsAg^{+}$ amphisomes, indicating HBV accumulation in amphisomes due to impaired exosome release.

In our previous study, HBV DNA, HBsAg, and HBcAg were co-fractioned with exosomes by western blot analysis.[15] In the present study, we aimed to enrich intact exosomes from cell culture media using polyethylene glycol precipitation and a commercially available total exosome isolation kit.[21] Sustainable detection of HBV DNA was achieved in fractions precipitated by different concentrations of polyethylene glycol incubation (Figure 5C) and those precipitated by the exosome kit (Figure 5D). Notably, GW4869 treatment also increased the HBV DNA level in the enriched exosome, suggesting a shared egress pathway for HBV and exosomes.

To comprehensively examine the involvement of amphisomes in HBV secretion, we employed a specific siRNA to target the *ATG5* gene in HepG2.2.15 cells (Figure 5E). Silencing of *ATG5* was confirmed by real-time RT-PCR detection of the target mRNA (Supplemental Figure S7, http://links.lww.com/HC9/B910). The knockdown of *ATG5* led to a significant reduction in the number of amphisomes and impaired HBV trafficking to amphisomes, underscoring the indispensable role of autophagy in amphisome formation and function. Despite combined treatment with GW4869, full restoration of amphisome numbers or their association with HBV was not achieved. *ATG5* silencing led to reduced LC3 immunofluorescence intensity and its association with HBsAg compared with siNC control. Nevertheless, the combined treatment with GW4869 recovered LC3 levels and partially increased the association of HBsAg with LC3. Notably, *ATG5* silencing did not affect the immunofluorescence intensity of CD63 or the association of HBsAg with CD63. These findings suggested that autophagosome formation is required for HBsAg trafficking to amphisomes. *ATG5* silencing slightly enhanced the suppression of HBV DNA release by GW4869 while having a marginal effect on HBsAg release and intracellular accumulation of HBsAg (Figure 5F). Collectively, targeting *ATG5* by siRNA interferes with amphisome formation and significantly reduces HBV DNA and HBsAg secretion, consistent with the proposed role of amphisomes in HBV secretion. Rab11 is a regulator of the fusion of autophagosomes and late endosomes/MVBs and

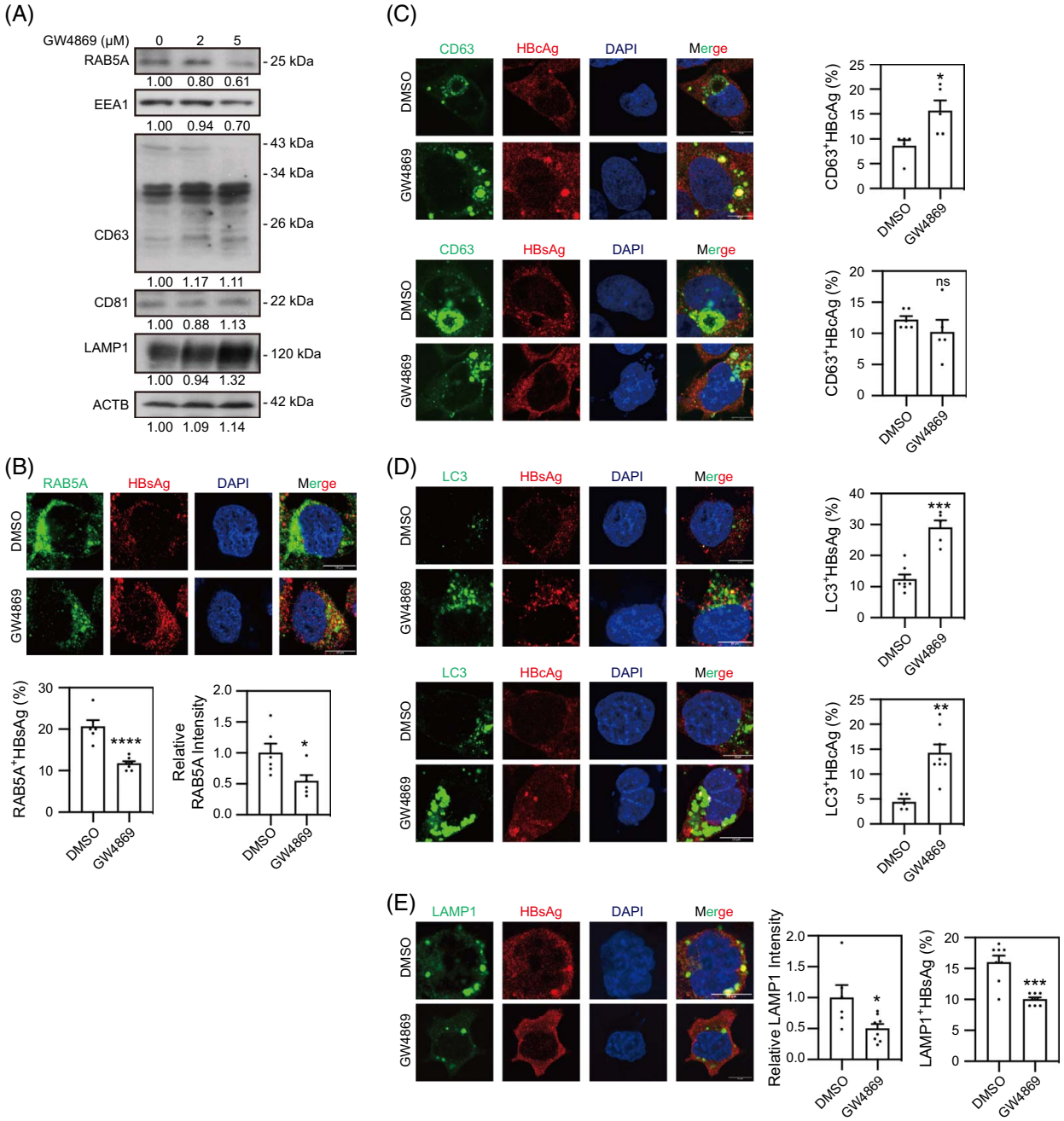

FIGURE 4 GW4869 treatment enhances the association of HBV with late endosomes/MVBs and autophagosomes. HepG2.2.15 cells were treated with 2 μM GW4869 for 48 hours. (A) The levels of intracellular RAB5A, EEA1, CD63, CD81, and LAMP1 were detected by western blot. The relative levels of indicated proteins were determined by quantifying the gray scales of bands using ImageJ software and ACTB as a loading control. (B) The colocalization of RAB5A with HBsAg, (C) CD63 with HBcAg or HBsAg, (D) LC3 with HBsAg or HBcAg, (E) and LAMP1 with HBsAg were detected. The fluorescence intensity of target proteins and the colocalization between target proteins were analyzed using ImageJ software. Scale bar: 10 μm. $^{*}p < 0.05$; $^{**}p < 0.01$; $^{***}p < 0.01$; $^{****}p < 0.0001$; and ns, not significant. Abbreviations: ACTB, beta-actin; EEA1, early endosome Ag 1; GW4869, N,N'-Bis[4-(4,5-dihydro-1H-imidazol-2-yl)phenyl]-3,3'-pht hal amide dihydrochloride); MVBs, multivesicular bodies; LAMP1, lysosomal-associated membrane protein 1.

participates in the release of HBV particles.[22] Similarly, Rab11 silencing decreased the amphisome formation (Supplemental Figure S8, http://links.lww.com/HC9/B910). This finding supports our conclusion that LC3^{+}CD63^{+} amphisomes are formed and associated with HBsAg.

nSMase, the target of GW4869, is required for HBV replication and trafficking

To validate the involvement of nSMase, a target of GW4869, in HBV replication and trafficking, hepatic cells were transfected with a specific siRNA targeting

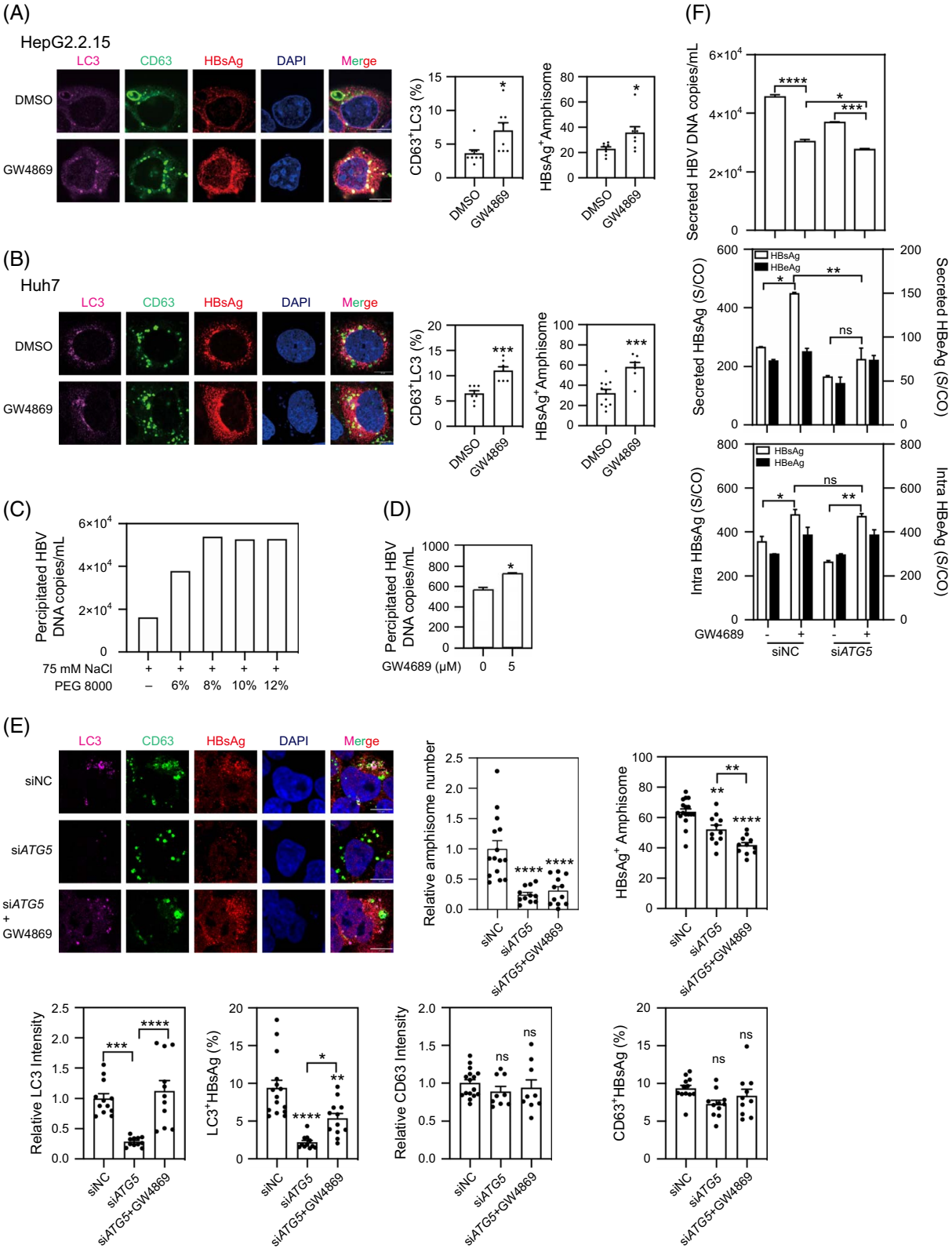

FIGURE 5 Amphisomes act as a platform for HBV secretion. (A) HepG2.2.15 cells were treated with 2 μM GW4869, and (B) pSM2-transfected Huh7 cells were treated with 1 μM GW4869 for 48 hours. The colocalization between target proteins was analyzed using ImageJ software. Scale bar: 10 μm. (C) HepG2.2.15 cells were cultured in 10% FBS media and treated with 2 μM and 5 μM GW4869 for 48 hours and without FBS for the last 24 hours. Total exosomes were precipitated using the PEG precipitation method and (D) total exosome isolation reagents. DNA was extracted from precipitated fractions using a DNA extraction kit. HBV DNA levels were quantified by real-time PCR. (E) HepG2.2.15 cells were transfected with 40 nM of si*ATG5,* and the transfection mixture was removed after 6 hours and treated with 2 μM GW4869 for 72 hours. The

fluorescence intensity of the target proteins and the colocalization between the target proteins were analyzed using ImageJ software. And (F) the secreted HBV DNA, HBsAg, and HBeAg, as well as intracellular HBsAg and HBeAg, were detected. $^{*}p < 0.05$; $^{**}p < 0.01$; $^{***}p < 0.01$; $^{****}p < 0.001$; and ns, not significant. Abbreviations: FBS, fetal bovine serum; GW4869, N,N'-Bis[4-(4,5-dihydro-1H-imidazol-2-yl)phenyl]-3,3'-pht hal amide dihydrochloride); PEG, polyethylene glycol; pSM2, HBV replication-competent plasmid.

nSMase, si*SMPD2* (sphingomyelin phosphodiesterase 2). The efficiency of si*SMPD2* in reducing *SMPD2* mRNA levels was confirmed through real-time RT-PCR (Supplemental Figure S9, http://links.lww.com/HC9/B910). Similar to the impact of GW4869 treatment, *SMPD2* silencing resulted in increased levels of intracellular HBV DNA and HBsAg, decreased levels of secreted HBV DNA, but without significant effects on HBV RNA levels in pSM2-transfected Huh7 cells and HepG2.2.15 cells (Figure 6A). Notably, *SMPD2* silencing significantly decreased HBV DNA secretion while promoting HBsAg secretion. *SMPD2* silencing had no measurable effect on HBV RNA expression. si*SMPD2* transfection increased the expression level of protein disulfide isomerase and its colocalization with HBsAg (Figure 6B), indicating the retention of HBsAg within the ER. *SMPD2* silencing decreased the expression level of RAB5A and its association with HBsAg (Figure 6C). Moreover, *SMPD2* silencing decreased the colocalization ratio of the autophagosome with LAMP1, resulting in increased LC3 expression levels. *SMPD2* silencing decreased the colocalization ratio of HBsAg with LAMP1 while increasing that with LC3, indicating less HBsAg transport to lysosomes for degradation and, instead, accumulation of HBsAg in autophagosomes (Figure 6D). In addition, *SMPD2* silencing increased the immunofluorescent intensity of CD63 and enhanced colocalization of HBsAg with CD63. The percentage of amphisomes increased from 13.3% to 26% after si*SMPD2* transfection, accompanied by an increase in the number of HBsAg^{+}Amphisome structures (from 41.4% to 51.6%) (Figure 6E). *SMPD2* silencing and GW4869 treatment had the same effect on HBV replication and trafficking. *SMPD2* overexpression increased the expression levels of Rab5a and CD63 and their association with HBsAg, which were reversed by GW4869 (Supplemental Figure S10, http://links.lww.com/HC9/B910). Thus, GW4869 modulates HBV replication and trafficking through neutral sphingomyelinase.

Silencing RAB27A and -B accumulate HBsAg in amphisomes

It is proposed that the secretion of certain cellular proteins by the autophagic pathway through the way of exosome release is dependent on *RAB27A*.[23,24] To gain further insight into the role of endosomal membrane trafficking in HBV release, *RAB27A* and *-B*, small GTPases controlling different steps of vesicular trafficking and exosome release were targeted. Both *RAB27A* and *-B* were found to colocalize with CD63 (Figure 7A). Gene silencing of RAB27A and -B was performed, with si*RAB27A*_7 and si*RAB27B*_4 selected for subsequent experiments due to their effective protein expression reduction by more than 50% (Supplemental Figure S11A, http://links.lww.com/HC9/B910).

Silencing *RAB27A* and *-B* individually increased the LC3 expression levels, with *RAB27A* silencing significantly increasing CD63 levels (Figure 7B), which was consistent with the known functions of *RAB27A* and *-B* in cargo export mediated by late endosomes/MVBs and autophagosomes. To examine the impact of *RAB27A* and *-B* silencing on autophagy flux, we combined their silencing with the chloroquine treatment. Combining *RAB27A* and *-B* silencing with chloroquine treatment did not significantly increase LC3-II levels (Supplemental Figure S11B, http://links.lww.com/HC9/B910), suggesting that the increased accumulation of autophagosomes by *RAB27A* and *-B* silencing is primarily a consequence of inhibiting autophagic degradation and secretion than the generation of new autophagosomes.

To assess the impact of *RAB27A* and *-B* silencing on HBV secretion, we measured intracellular and extracellular levels of HBV DNA and HBsAg. Silencing *RAB27A* increased intracellular HBV DNA levels while reducing released HBV DNA and HBsAg in supernatants (Figure 7C). Silencing *RAB27B* had minimal effect on intracellular HBV DNA levels and did not influence the secreted HBV DNA and HBsAg levels. More interestingly, the subcellular distribution of HBsAg also changed. IF images indicated that HBsAg exhibited a homogenous distribution throughout the cytoplasm, while *RAB27A* and *-B* silencing resulted in perinuclear accumulation (Figure 7D). We further investigated the association of HBsAg with endosomes and autophagosomes. Silencing *RAB27A* increased early endosome number and HBsAg colocalization, whereas silencing *RAB27B* did not affect HBsAg's association with early endosomes (Figure 7E). Consistent with western blot results, IF demonstrated a notable elevation in LC3 expression levels upon silencing *RAB27A* and *-B*. si*RAB27A* increased CD63 levels. Silencing *RAB27A* and *-B* increased HBsAg colocalization with autophagosomes but reduced its colocalization with late endosomes/MVBs. The percentage of HBsAg^{+} amphisome increased (Figure 7F), consistent with *RAB27*'s roles in the amphisome release.[25] Intensity plots of the proteins analyzed within the cells also revealed that silencing *RAB27A* and *-B* caused a perinuclear accumulation of HBsAg^{+}Amphisome structure. Again, amphisomes are involved in HBV production and secretion.

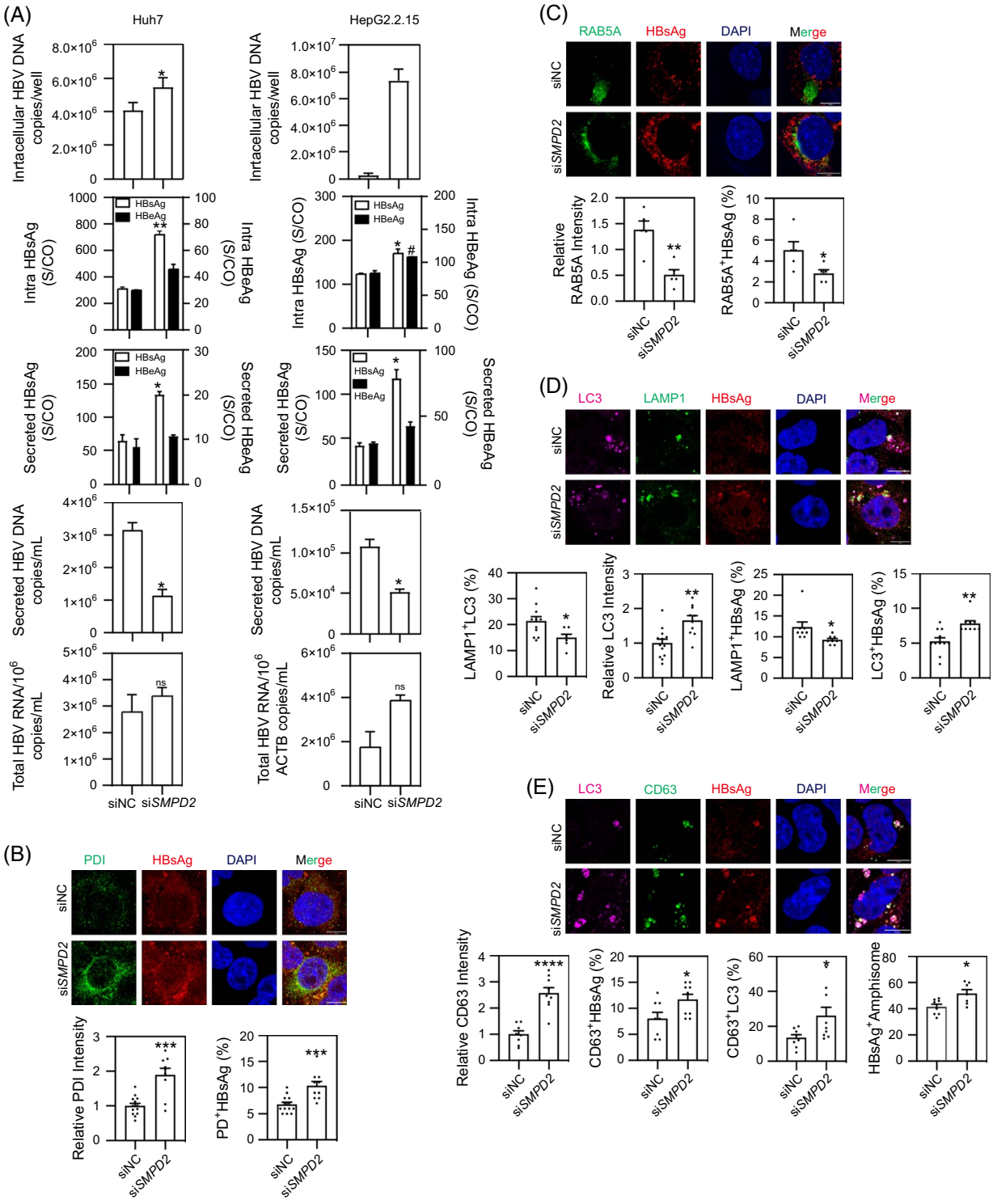

FIGURE 6 GW4869 mediates HBV replication and trafficking by impeding the activity of neutral sphingomyelinase. (A) Huh7 cells were cotransfected with pSM2 and si*SMPD2*. HepG2.2.15 cells were transfected with si*SMPD2*. Cells were harvested after 72 hours. siNC acted as a control. The levels of intracellular and secreted HBV DNA, secreted and intracellular HBsAg and HBeAg, and total HBV RNAs were detected. (B–E) HepG2.2.15 cells were transfected with 40 nM siNC or siSMPD2 for 72 hours. The expression levels of (B) PDI, (C) RAB5A, (D) LC3 and LAMP1, (E) CD63, and the colocalization between target proteins were analyzed using ImageJ software. Scale bar: 10 μm. $^{*,\#}p < 0.05$; $^{**}p < 0.01$; $^{***}p < 0.001$; $^{****}p < 0.0001$, and ns, not significant. Abbreviations: GW4869, N,N'-Bis[4-(4,5-dihydro-1H-imidazol-2-yl)phenyl]-3,3'-pht hal amide dihydrochloride; LAMP1, lysosomal-associated membrane protein 1; PDI, protein disulfide isomerase; pSM2, HBV replication-competent plasmid; SMPD2, sphingomyelin phosphodiesterase 2.

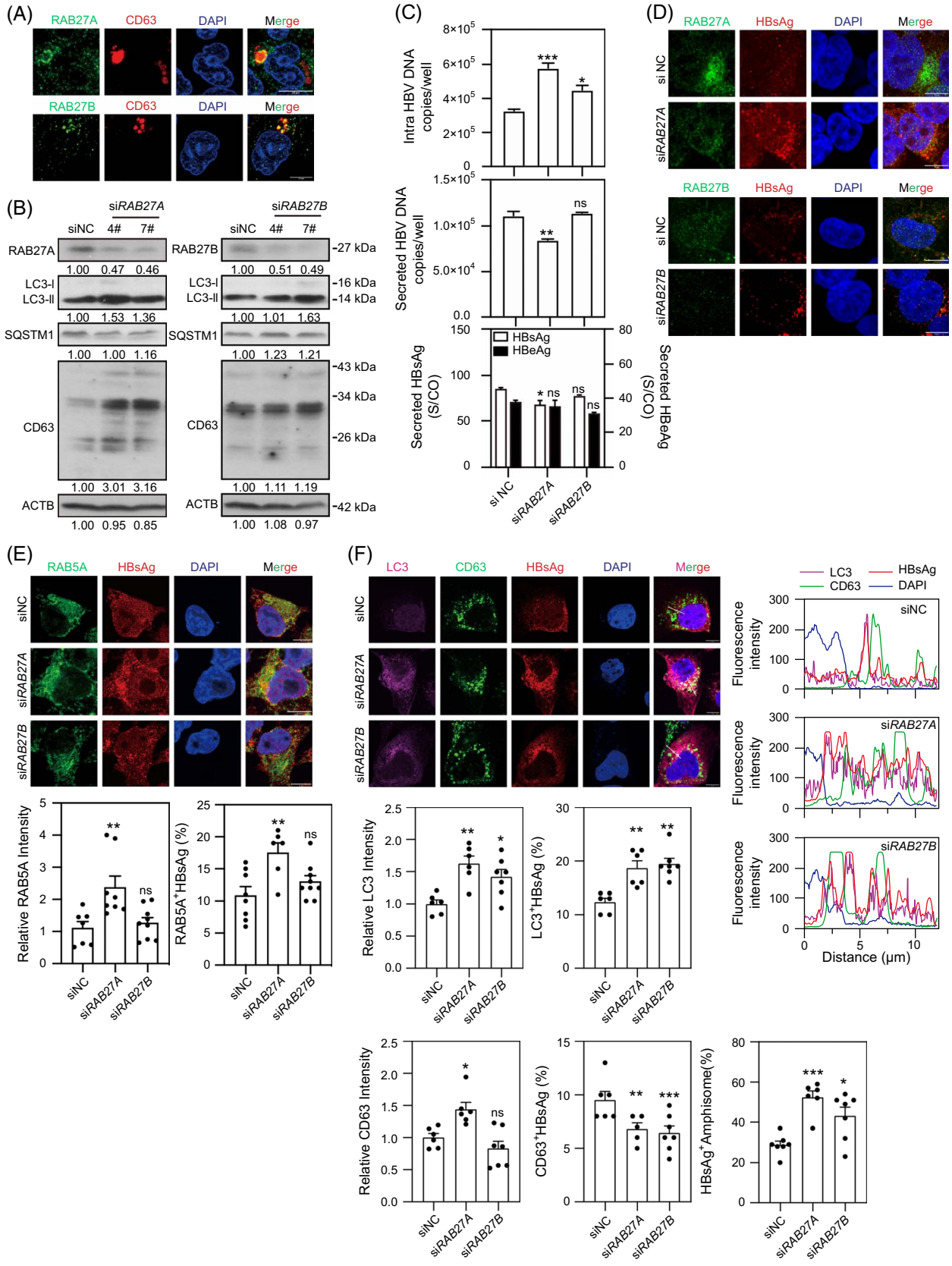

FIGURE 7 *RAB27A* and *RAB27B* control HBV secretion and distribution. (A) HepG2.2.15 cells cultured at 10% FBS medium for 48 hours were subjected to IF. The distributions of CD63 with *RAB27A* or *-B* were imaged. (B–F) HepG2.2.15 cells were transfected with 40 nM siNC, si*RAB27A*, and si*RAB27B* for 72 hours. (B) The expression levels of RAB27A, RAB27B, LC3, p62, and CD63 were determined by western blot. The relative levels of indicated proteins were determined by quantifying the gray scales of bands using ImageJ software and ACTB as a loading

control. (C) The intracellular and secreted HBV DNA and the secreted HBsAg and HBeAg levels were detected. (D) The distributions of HBsAg with *RAB27A* or *-B* were imaged. The expression levels of (E) RAB5A, (F) LC3, and CD63, and the colocalization between target proteins were analyzed using ImageJ software. The distribution of LC3, CD63, and HBsAg was analyzed by determining their intensity profiles along the white arrows using ImageJ software. Scale bar: 10 μm. $^{*}p < 0.05$; $^{**}p < 0.01$; $^{***}p < 0.001$; and ns, not significant. Abbreviations: ACTB, beta-actin; FS, fetal bovine serum; IF, immunofluorescence; p62, sequestosome 1.

DISCUSSION

Here we demonstrate that amphisomes act as a platform for HBV secretion. Previous work has revealed important interconnections between autophagy and endosomes. Previously, we showed that ER stress promotes HBV production by enhancing the use of the autophagosome/MVB axis.[15] The disruption of endosomal trafficking redirects HBsAg and HBV virions to autophagosomes for degradation.[7] In addition, RAB11 silencing disturbs the fusion of autophagosomes and MVBs, leading to reduced HBV virion release.[22] Our findings provided evidence for a previously unexplored function of amphisomes in the HBV life cycle.

Some studies show that GW4869 inhibits HBV-containing exosome secretion, thereby affecting HBV release and infection.[8,9] However, it remains unclear whether GW4869 also affects the autophagic pathway. In the present study, we have examined how GW4869-mediated inhibition of exosome biogenesis impacts autophagy and HBV replication. Our results show that GW4869 disrupts the endosomal pathway, accumulates HBV in the ER, triggers autophagy in a feedback loop, accelerates amphisome formation, and arrests HBV in the amphisome. To our knowledge, this is the first demonstration of GW4869's effect on the distribution and trafficking of HBV components in the endosomal and autophagic pathways, resulting in decreased HBV release.

In a stable HBV replication system like HepG2.2.15 cells, the ongoing high-level viral replication provides a steady pool of HBV proteins. Thus, a large amount of HBsAg accumulated in the cells may be exported through the ER-Golgi pathway in the presence of GW4869. In contrast, GW4869 treatment has little to no effect or even reduces HBsAg secretion in the de novo synthesis models, including pSM2-transfected Huh7 cells and HBV-infected PHHs, as HBsAg levels are low at the beginning and will be high at late time points.

Our study also suggests that Sphingomyelin Phosphodiesterase 2 (SMPD2) plays a crucial role in the modulation of HBV trafficking and release by GW4869. Similar to GW4869 treatment, SMPD2 silencing significantly increased the secretion of HBsAg through the ER-Golgi pathway, resulting in higher levels of HBsAg in cell culture supernatants. The disruption of the late endosome/exosome secretion pathway, coupled with the activation of autophagy, led to increased intracellular accumulation of HBsAg. Thus, SMPD2 silencing yielded results consistent with those observed following GW4869 treatment, validating the involvement of SMPD2 in regulating HBV replication and transport as the GW4869 target. nSMases are the important enzymes responsible for the breakdown of sphingomyelin into ceramide in exosome biogenesis.[26,27] Depletion of nSMase2 impairs the incorporation of endogenous LC3 into endosomes, thereby impeding LC3-dependent EV loading and secretion.[28] Thus, the accumulation of autophagosomes induced by GW4869 is also dependent on nSMase disruption. These data show the significance of nSMase in coordinating endosomal and autophagic pathways.

Recent studies have revealed that HBV core particles localize to autophagic membranes and productively replicate HBV genomes.[22] Here, we confirmed the colocalization of HBsAg and HBcAg with LC3. Furthermore, an increased colocalization ratio after GW4869 treatment indicated enhanced recruitment of HBsAg and HBcAg to autophagosomes when the endosomal pathway was impaired. This is consistent with our previous finding that autophagy constitutes an alternative secretion pathway.[7]

We observed that the decrease in early endosomes did not directly inhibit late endosome formation but instead altered the morphology of late endosomes/MVBs. The number of late endosomes could remain relatively constant due to the balance among maturation, degradation, recycling rates, and other compensatory mechanisms, which stabilizes the overall late endosome pool.

RAB27A and *-B* are 2 GTPase proteins with high sequence similarity,[29] yet they exhibit distinct functions in HBV trafficking and release. Both *RAB27A* and *-B* silencing caused the cellular accumulation of HBsAg in amphisomes, while the secretion of HBV DNA and HBsAg was only suppressed in *RAB27A*-silenced cells. This finding aligns with previous findings by Matias et al,[12] who found that *RAB27A* and *-B* control different steps of late endosome/MVB formation and exosome release. Specifically, *RAB27A* is required for membrane fusion and cargo release, while *RAB27B* probably regulates MVB motility. *RAB27B* silencing led to a modest accumulation of HBV components, yet it did not sufficiently initiate substantial ER stress (Supplemental Figure S12, http://links.lww.com/HC9/B910). Consequently, this condition resulted in the deceleration of HBsAg transportation towards endosomes and autophagosomes but accumulated in the amphisomes.

TABLE 1 List of antibodies

Product name	Company
Anti-RAB5A Rabbit antibody	Cell Signaling Technology, 46449S
Anti-EEA1 Rabbit antibody	Cell Signaling Technology, 48453S
Anti-CD63 Mouse antibody	Santa Cruz Biotechnology, sc-5275
Anti-SQSTM1 Rabbit antibody	Cell Signaling Technology, 5114S
Anti-LC3B Rabbit antibody	Cell Signaling Technology, 3868S
Anti-LAMP1 Mouse antibody	Cell Signaling Technology, 15665S
Anti-ACTB Mouse antibody	Sigma-Aldrich, A5441
Anti-HBsAg Mouse antibody	ZSGB-BIO, ZM-0122
Anti-HBcAg Rabbit antibody	ZSGB-BIO, ZA-0121
Anti-PDI Rabbit antibody	Cell Signaling Technology, 3501S
Anti-HSPA5 Rabbit antibody	Cell Signaling Technology, 3177S
Anti-EIF2A Rabbit antibody	Cell Signaling Technology, 9722S
Anti-Phospho-EIF2A Rabbit antibody	Cell Signaling Technology, 9721S
Anti-ATF6 Rabbit antibody	Cell Signaling Technology, 65880S
Anti-AKT Rabbit antibody	Cell Signaling Technology, 9272S
Anti-Phospho-AKT Rabbit antibody	Cell Signaling Technology, 9271S
Anti-MTOR Rabbit antibody	Cell Signaling Technology, 2972S
Anti-Phospho-MTOR Rabbit antibody	Cell Signaling Technology, 2971S
Anti-RPS6KB Rabbit antibody	Cell Signaling Technology, 9202S
Anti-Phospho-RPS6KB Rabbit antibody	Cell Signaling Technology, 9209S
Anti-ULK1 Rabbit antibody	Cell Signaling Technology, 8054S
Anti-Phospho-ULK1 Rabbit antibody	Cell Signaling Technology, 14202S
Anti-HBsAg Horse antibody	Abcam, ab9193
Anti-LC3B Mouse antibody	Cell Signaling Technology, 83506S
Anti-RAB27A Rabbit antibody	Cell Signaling Technology, 69295S
Anti-RAB27B Rabbit antibody	Cell Signaling Technology, 17572S
Anti-Rabbit IgG, HRP-linked antibody	Cell Signaling Technology, 7074
Anti-Mouse IgG, HRP-linked antibody	Cell Signaling Technology, 7076
Alexa Fluor 488-conjugated Goat anti-Rabbit IgG (H+L)	Cell Signaling Technology, 4412
Alexa Fluor 488-conjugated Goat anti-Mouse IgG (H+L)	Cell Signaling Technology, 4408
Alexa Fluor 594-conjugated Goat anti-Mouse IgG (H+L)	Cell Signaling Technology, 8890
Alexa Fluor 594-conjugated Goat anti-Rabbit IgG (H+L)	Cell Signaling Technology, 8889
Alexa Fluor 594-conjugated Rabbit anti-Horse IgG (H+L)	Jackson ImmunoResearch, 308-585-003
Alexa Fluor 647-conjugated Goat anti-Rabbit IgG (H+L)	Cell Signaling Technology, 4414

Abbreviations: ACTB, beta-actin; AKT, Protein kinase B; ATF6, activating transcription factor 6; EEA1, early endosome Ag 1; EIF2A, eukaryotic translation initiation factor 2A; LAMP1, lysosomal-associated membrane protein 1; MTOR, mechanistic target of rapamycin kinase; PDI, protein disulfide isomerase; RPS6KB, ribosomal protein S6 Kinase B1; ULK1, UNC-51-like kinase 1.

Conventionally, amphisomes mediate the delivery of cellular cargos for lysosomal degradation. The unconventional secretory function of amphisomes is only found in neurodegenerative disorders[30–32] and ANXA2 secretion in lung epithelial cells.[33] In this study, we visualized the amphisome and its association with HBsAg. Treatment with GW4869 and silencing of *RAB27A* and *-B* lead to an accumulation of $HBsAg^+LC3^+CD63^+$ structures, showing the involvement of amphisomes in HBV replication and release.

In conclusion, our results demonstrate that the autophagy-late endosomes/MVBs-exosome axis regulates HBV replication and release. We also provide strong evidence for the involvement of amphisome as a platform for HBV release.

AUTHOR CONTRIBUTIONS

Jia Li conducted experiments and prepared the manuscript. Thekla Kemper, Ruth Broering, Yong Lin, and Xueyu Wang contributed to the reagent supply and

provided technical support. Mengji Lu contributed to the conception, supervision, and revision of the manuscript.

FUNDING INFORMATION

This work was supported by grants from Deutsche Forschungsgemeinschaft (RTG1949/2, Lu 669/12-1 and Lu 669/13-1 to Mengji Lu, 398762835 and 450164446 to Ruth Broering).

CONFLICTS OF INTEREST

The authors report no conflicts of interest.

REFERENCES

1. Tu T, Block JM, Wang S, Cohen C, Douglas MW. The lived experience of chronic hepatitis B: A broader view of its impacts and why we need a cure. Viruses. 2020;12:515.
2. Bruss V. Hepatitis B virus morphogenesis. World J Gastroenterol. 2007;13:65–73.
3. Hu J, Liu K. Complete and incomplete hepatitis B virus particles: Formation, function, and application. Viruses. 2017;9:56.
4. Watanabe T, Sorensen EM, Naito A, Schott M, Kim S, Ahlquist P. Involvement of host cellular multivesicular body functions in hepatitis B virus budding. Proc Natl Acad Sci USA. 2007;104:10205–10.
5. Jiang B, Himmelsbach K, Ren H, Boller K, Hildt E. Subviral hepatitis B virus filaments, like infectious viral particles, are released via multivesicular bodies. J Virol. 2015;90:3330–41.
6. Lin Y, Zhao Z, Huang A, Lu M. Interplay between cellular autophagy and hepatitis B virus replication: A systematic review. Cells. 2020;9:2101.
7. Wang X, Wei Z, Lan T, He Y, Cheng B, Li R, et al. CCDC88A/GIV promotes HBV replication and progeny secretion via enhancing endosomal trafficking and blocking autophagic degradation. Autophagy. 2022;18:357–74.
8. Wu Q, Glitscher M, Tonnemacher S, Schollmeier A, Raupach J, Zahn T, et al. Presence of intact hepatitis B virions in exosomes. Cell Mol Gastroenterol Hepatol. 2023;15:237–59.
9. Sanada T, Hirata Y, Naito Y, Yamamoto N, Kikkawa Y, Ishida Y, et al. Transmission of HBV DNA mediated by ceramide-triggered extracellular vesicles. Cell Mol Gastroenterol Hepatol. 2017;3:272–83.
10. Catalano M, O'Driscoll L. Inhibiting extracellular vesicles formation and release: A review of EV inhibitors. J Extracell Vesicles. 2020;9:1703244.
11. Zhang Q, Qu Y, Zhang Q, Li F, Li B, Li Z, et al. Exosomes derived from hepatitis B virus-infected hepatocytes promote liver fibrosis via miR-222/TFRC axis. Cell Biol Toxicol. 2023;39:467–81.
12. Ostrowski M, Carmo NB, Krumeich S, Fanget I, Raposo G, Savina A, et al. Rab27a and Rab27b control different steps of the exosome secretion pathway. Nat Cell Biol. 2010;12:19–30; sup pp 11-13.
13. Chen TC, Hsieh CH, Sarnow P. Supporting role for GTPase Rab27a in hepatitis C virus RNA replication through a novel miR-122-mediated effect. PLoS Pathog. 2015;11:e1005116.
14. Nagashima S, Jirintai S, Takahashi M, Kobayashi T, Tanggis, Nishizawa T, et al. Hepatitis E virus egress depends on the exosomal pathway, with secretory exosomes derived from multivesicular bodies. J Gen Virol. 2014;95(Pt 10):2166–75.
15. Wang X, Wei Z, Cheng B, Li J, He Y, Lan T, et al. Endoplasmic reticulum stress promotes HBV production by enhancing use of the autophagosome/multivesicular body axis. Hepatology. 2022;75:438–54.
16. Li J, Liu Y, Wang Z, Liu K, Wang Y, Liu J, et al. Subversion of cellular autophagy machinery by hepatitis B virus for viral envelopment. J Virol. 2011;85:6319–33.
17. Lin Y, Deng W, Pang J, Kemper T, Hu J, Yin J, et al. The microRNA-99 family modulates hepatitis B virus replication by promoting IGF-1R/PI3K/Akt/mTOR/ULK1 signaling-induced autophagy. Cell Microbiol. 2017;19:e12709.
18. Berg TO, Fengsrud M, Strømhaug PE, Berg T, Seglen PO. Isolation and characterization of rat liver amphisomes. Evidence for fusion of autophagosomes with both early and late endosomes. J Biol Chem. 1998;273:21883–92.
19. Fader CM, Colombo MI. Autophagy and multivesicular bodies: Two closely related partners. Cell Death Differ. 2009;16:70–8.
20. Ganesan D, Cai Q. Understanding amphisomes. Biochem J. 2021;478:1959–76.
21. Ludwig AK, De Miroschedji K, Doeppner TR, Börger V, Ruesing J, Rebmann V, et al. Precipitation with polyethylene glycol followed by washing and pelleting by ultracentrifugation enriches extracellular vesicles from tissue culture supernatants in small and large scales. J Extracell Vesicles. 2018;7:1528109.
22. Chu JYK, Chuang YC, Tsai KN, Pantuso J, Ishida Y, Saito T, et al. Autophagic membranes participate in hepatitis B virus nucleocapsid assembly, precore and core protein trafficking, and viral release. Proc Natl Acad Sci USA. 2022;119:e2201927119.
23. Solvik TA, Nguyen TA, Tony Lin YH, Marsh T, Huang EJ, Wiita AP, et al. Secretory autophagy maintains proteostasis upon lysosome inhibition. J Cell Biol. 2022;221:e202110151.
24. Xu J, Yang KC, Go NE, Colborne S, Ho CJ, Hosseini-Beheshti E, et al. Chloroquine treatment induces secretion of autophagy-related proteins and inclusion of Atg8-family proteins in distinct extracellular vesicle populations. Autophagy. 2022;18:2547–60.
25. Hassanpour M, Rezabakhsh A, Rezaie J, Nouri M, Rahbarghazi R. Exosomal cargos modulate autophagy in recipient cells via different signaling pathways. Cell Biosci. 2020;10:92.
26. Guo BB, Bellingham SA, Hill AF. The neutral sphingomyelinase pathway regulates packaging of the prion protein into exosomes. J Biol Chem. 2015;290:3455–67.
27. Trajkovic K, Hsu C, Chiantia S, Rajendran L, Wenzel D, Wieland F, et al. Ceramide triggers budding of exosome vesicles into multivesicular endosomes. Science. 2008;319:1244–7.
28. Leidal AM, Huang HH, Marsh T, Solvik T, Zhang D, Ye J, et al. The LC3-conjugation machinery specifies the loading of RNA-binding proteins into extracellular vesicles. Nat Cell Biol. 2020;22:187–99.
29. Izumi T. In vivo Roles of Rab27 and Its Effectors in Exocytosis. Cell Struct Funct. 2021;46:79–94.
30. Duran JM, Anjard C, Stefan C, Loomis WF, Malhotra V. Unconventional secretion of Acb1 is mediated by autophagosomes. J Cell Biol. 2010;188:527–36.
31. Minakaki G, Menges S, Kittel A, Emmanouilidou E, Schaeffner I, Barkovits K, et al. Autophagy inhibition promotes SNCA/alpha-synuclein release and transfer via extracellular vesicles with a hybrid autophagosome-exosome-like phenotype. Autophagy. 2018;14:98–119.
32. Zhang M, Kenny SJ, Ge L, Xu K, Schekman R. Translocation of interleukin-1beta into a vesicle intermediate in autophagy-mediated secretion. eLife. 2015;4:e11205.
33. Chen YD, Fang YT, Cheng YL, Lin CF, Hsu LJ, Wang SY, et al. Exophagy of annexin A2 via RAB11, RAB8A and RAB27A in IFN-gamma-stimulated lung epithelial cells. Sci Rep. 2017;7:5676.

How to cite this article: Li J, Kemper T, Broering R, Lin Y, Wang X, Lu M. Amphisome plays a role in HBV production and release through the endosomal and autophagic pathways. Hepatol Commun. 2025;9:e0654. https://doi.org/10.1097/HC9.0000000000000654